Molecular Simulation, Vol. 29 (10–11), October–November 2003, pp. 619–626

Taylor & Francis
Taylor & Francis Group

Formation of Quasi Two-dimensional Bilayer Ice in Hydrophobic Slits: A Possible Candidate for Ice XIII?

J. BAI[a], X.C. ZENG[a,*], K. KOGA[b] and H. TANAKA[c]

[a]*Department of Chemistry, University of Nebraska-Lincoln, Lincoln, NE 68588, USA;* [b]*Department of Chemistry, Cornell University, Ithaca, NY 14853, USA;* [c]*Department of Chemistry, Okayama University, Okayama 700-8530, Japan*

(Received October 2002; In final form February 2003)

We performed molecular dynamics simulations of water confined to hydrophobic slit nanopores. Two five-site potential models of water were employed: the ST2 model and the TIP5P model. The simulations confirm our previous simulation results on basis of the four-site TIP4P model of water, that is, upon cooling the confined liquid water may undergo a first-order phase transition to either a bilayer crystalline ice phase or to a bilayer amorphous ice. The selection of the bilayer crystalline phase occurs at the constant normal pressure condition whereas the selection of the bilayer amorphous ice phase is likely to occur at the fixed pore-width condition. This computer-simulation generated ice form, if confirmed by crystallographic or spectroscopic experiments, may be a candidate for "ice XIII", provided that purely quasi two-dimensional ice forms (metastable in vacuum) can be viewed as a stand-alone solid phase of ice.

Keywords: Ice XIII; Bilayer ice; ST2; TIP5P

INTRODUCTION

Three-dimensional bulk ice displays a rich phase diagram [1]. Under pressure, bulk ice can exhibit many solid-phase transformations, which include a variety of metastable crystalline phases and amorphous phases [2]. To date, 13 forms of bulk crystalline ice have been found either in nature or in laboratories. Ice I alone has two polymorphs, one is the hexagonal ice I_h (i.e. the normal ice) and another is the metastable cubic ice I_c. The latest metastable form of ice, ice XII, was uncovered in 1998 [3].

It is also known that new phases can emerge in microscopically confined environments [4–6] such as slit pores. The special character of confined systems stems from their spatial inhomogeneity. Forced to pack into spaces severely constricted by two confining walls, molecules in the vicinity of the fluid–wall interface tend to arrange themselves in layers parallel with the interface. The resulting oscillations in local density are reflected in properties of the confined phase that can differ drastically from those of the bulk counterpart. Some of the new phase behavior, such as wetting and layering transitions, is due solely to the presence of the interface; others, such as capillary freezing, can be regarded "simply" as bulk behaviors modified by the presence of the confining walls.

Recently, we reported computer simulation evidences of the possible existence of a new quasi two-dimensional (Q2D) form of crystalline ice [7–10] and a Q2D amorphous ice [11] for water confined to a hydrophobic nanoslit. Both types of transition—liquid water to Q2D ice and amorphous ice—are strongly first-order. In our previous MD simulations, the four-site TIP4P water model was employed. In these MD simulations, we used two ways to control the confinement conditions. In one case [7–10], we allowed the two confining walls to be movable in order to achieve a constant normal pressure condition. In another case, we fixed the distance in between the two walls while allowing the lateral area of the simulation cell to change in order to achieve a constant lateral pressure condition. In the former case, the bilayer ice crystal was observed upon cooling whereas in the latter case the amorphous bilayer ice was observed. Presumably, by fixing the pore width gives rise to certain "frustration" in

*Corresponding author.

ISSN 0892-7022 print/ISSN 1029-0435 online © 2003 Taylor & Francis Ltd
DOI: 10.1080/0892702031000103158

the normal direction (perpendicular to the walls) to prevent the formation of perfect crystal. Furthermore, the change in the lateral area during the simulation seems to allow the system to be more easily "trapped" in the metastable amorphous state. Could the formation of these Q2D ice and amorphous ice be an artifact of the TIP4P [12] model of water? To address this question, we have performed a new set of MD simulations with other popular models of water, the five-site ST2 model [13] and TIP5P model [14]. Note that the four-site TIP4P model has a planar structure whereas both ST2 and TIP5P models are tetrahedral-like in geometry. The ST2 model is amongst the earliest molecular models of water, developed by Stillinger and Raman in the 1970s, and is known to be strongly tetrahedral. It is a modified version of the BNS model [13]. The TIP5P is the latest model in the TIP series developed by Jorgensen and coworkers. One improvement over the previous TIP models is that the TIP5P can quantitatively reproduce the temperature at which the maximum density occurs.

MODELS AND METHODS

The five sites of ST2 and TIP5P model consist of one oxygen (O), two hydrogen (H) and two virtual sites (M). For the ST2 model, the bond length of O—M is 0.8 Å and O—H is 1.0 Å. Both the ∠MOM and ∠HOH angles are tetrahedral-like (109.47°). The oxygen site has Lennard–Jones (LJ) parameters, $\epsilon = 0.07575$ kcal/mol and $\sigma = 3.10$ Å. Two hydrogen sites carry a charge, $q = 0.2357$e. A negative charge $-q$ is assigned to each virtual site (M). The ST2 potential function involves a short-range switching function that smoothly cuts off the potential at the O—O distance (r_{oo}) of two molecules. At distances less than $r_{oo} = 3.1287$ Å, the switching function is active but it completely cuts off the interaction at $r_{oo} = 2.0106$ Å. In contrast, no short-range switching function is involved in the TIP5P potential function. For TIP5P, the bond length of O—H is 0.9572 Å and O—M is 0.7 Å. The angle ∠MOM is the same as ST2 but ∠HOH is 104.52°. The H site has a charge, $q = 0.241$e. The M site has a negative charge $-q$. The LJ parameters of O site are $\epsilon = 0.16$ kcal/mol and $\sigma = 3.12$ Å. The wall is a smooth planar wall, and the wall–oxygen site interaction is taken to be the nonpolar 9–3 LJ interaction [7,15] with the LJ parameters $\epsilon = 1.1827$ kcal/mol and $\sigma = 2.4782$ Å. Thus, the wall is hydrophobic.

As in our previous MD simulations, we used two kinds of confined systems [7,11]. In both systems, water was confined in between two plane-parallel smooth solid walls. In the first system (system I) a constant normal-pressure condition was imposed [7] while the lateral area of the system was fixed. To this end, the distance in between the two planar walls was allowed to change. In the second system (system II), the constant lateral-pressure condition was imposed [11] while the distance in between the two walls was fixed. The lateral area of the simulation cell was allowed to vary in order to achieve the constant lateral-pressure condition. For both systems, the periodic boundary conditions were applied in lateral directions (x and y) in parallel with the two walls.

In system I, the simulation cell contained 192 water molecules.[†] The planar wall is a 34.16×28.797 Å^2 rectangular prism (for TIP5P) or 33.55×29.06 Å^2 prism (for ST2). The normal pressure was fixed at 1 GPa. The MD simulation started at a temperature of 330 K. We lowered the system temperature in steps (typically 10 K in temperature change) from 330 K until a freezing transition was observed. We then raised the temperature sequentially (also in steps) up to the point where a melting transition was observed. Smaller temperature steps (1–4 K in temperature change) were used near the transition point. At each temperature, the MD run time was in between 2 and 15 ns. Note that the MD timestep is 0.4 fs. For TIP5P model, longer MD times up to 40 ns were used near the transition point, whereas for ST2 model it was found that 4 ns MD time was sufficient to observe the 2D ice formation process near the transition point, due to the strongly tetrahedral character of ST2 model.

In system II, the distance between the two walls was fixed. The pore space in the normal direction (z direction) just accommodates about two layers of water molecules. The simulation cell contained 200 water molecules. The lateral pressure was fixed at 0.1 MPa. As for system I, the temperature of system II was lowered in steps starting from 330 towards 250 K, and then raised sequentially until a melting transition was observed.

RESULTS AND DISCUSSION

Figure 1a shows the temperature dependence of the quenched potential energy (QPE) for both ST2 and TIP5P water in system I. The QPE was obtained by using the steepest descent method to map a few tens

[†]Previously we have studied effects of system size [8,11] and periodic-boundary conditions [9,10] for the TIP4P model. The largest system size studied consisted of 960 water molecules [11]. It was found that the final hexagonal morphology of 2D bilayer ice is not dependent on the system size.

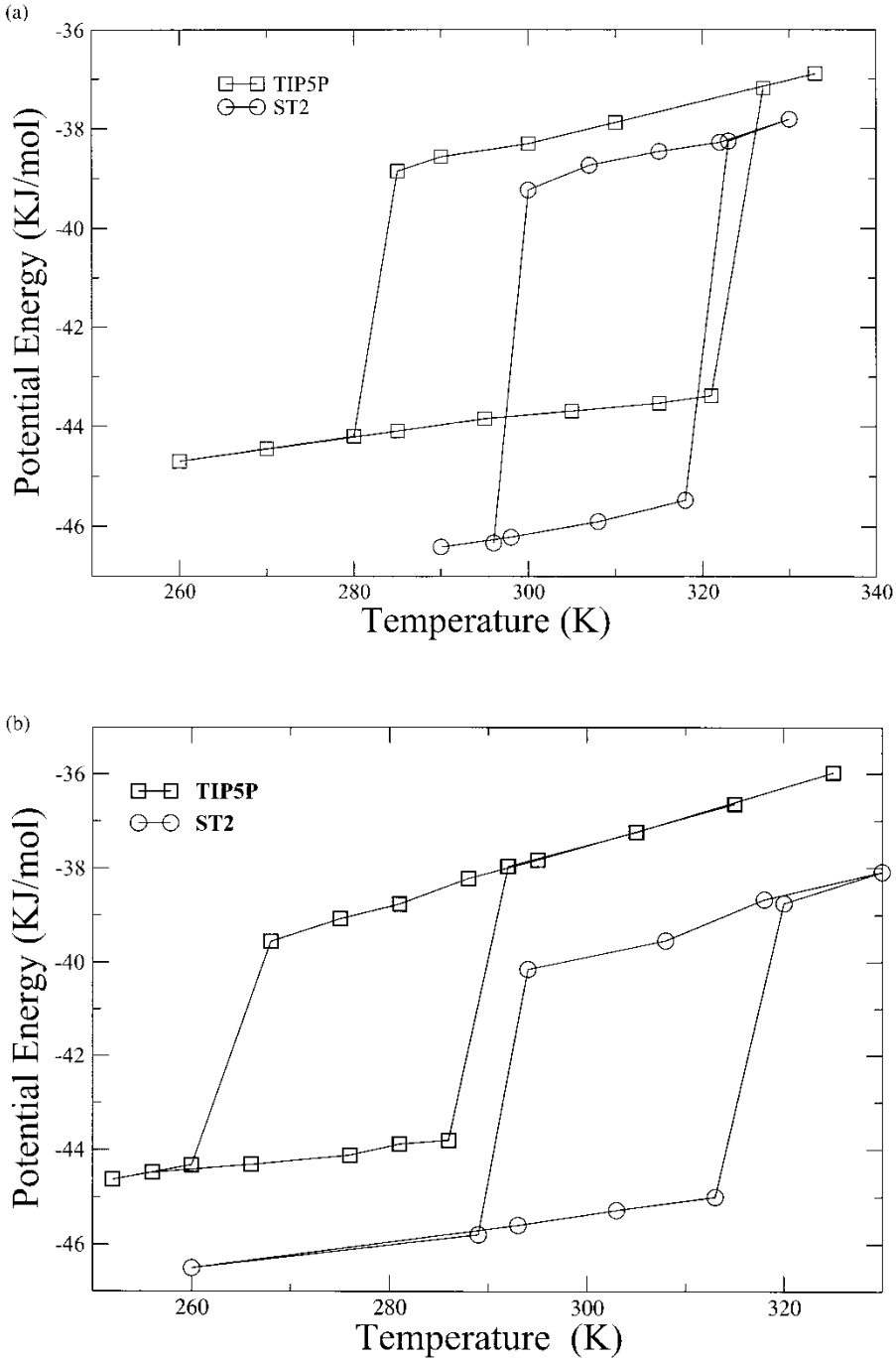

FIGURE 1 Temperature dependence of the QPE in (a) system I and (b) system II.

of instantaneous configurations of the confined water onto their inherent structure [16]. Note that the QPE includes a vibrational energy $3RT$ where R is the gas constant and T is the temperature of the system, but excludes the interaction potential energy between water and the walls. In system I, as the temperature was lowered the QPE exhibits a sharp drop at 293 K for ST2 and at 280 K for TIP5P. In the heating process, a sharp jump in the QPE occurred at 320 K for ST2 and at 327 K for TIP5P. This hysteresis-loop behavior demonstrates the appearance of a strong first-order phase transition in the confined system. Figure 1b shows the temperature dependence of the QPE for system II. Again, a similar hysteresis-loop behavior was observed. Figure 2 displays the quenched configuration of the TIP5P water prior to and after the phase transition in the system I. As shown in Fig. 2b,c, the quenched configuration in system I is a bilayer of hexagonal ice crystal, whereas in system II it is a polygonal amorphous bilayer ice. Both types of phase transition were observed previously on

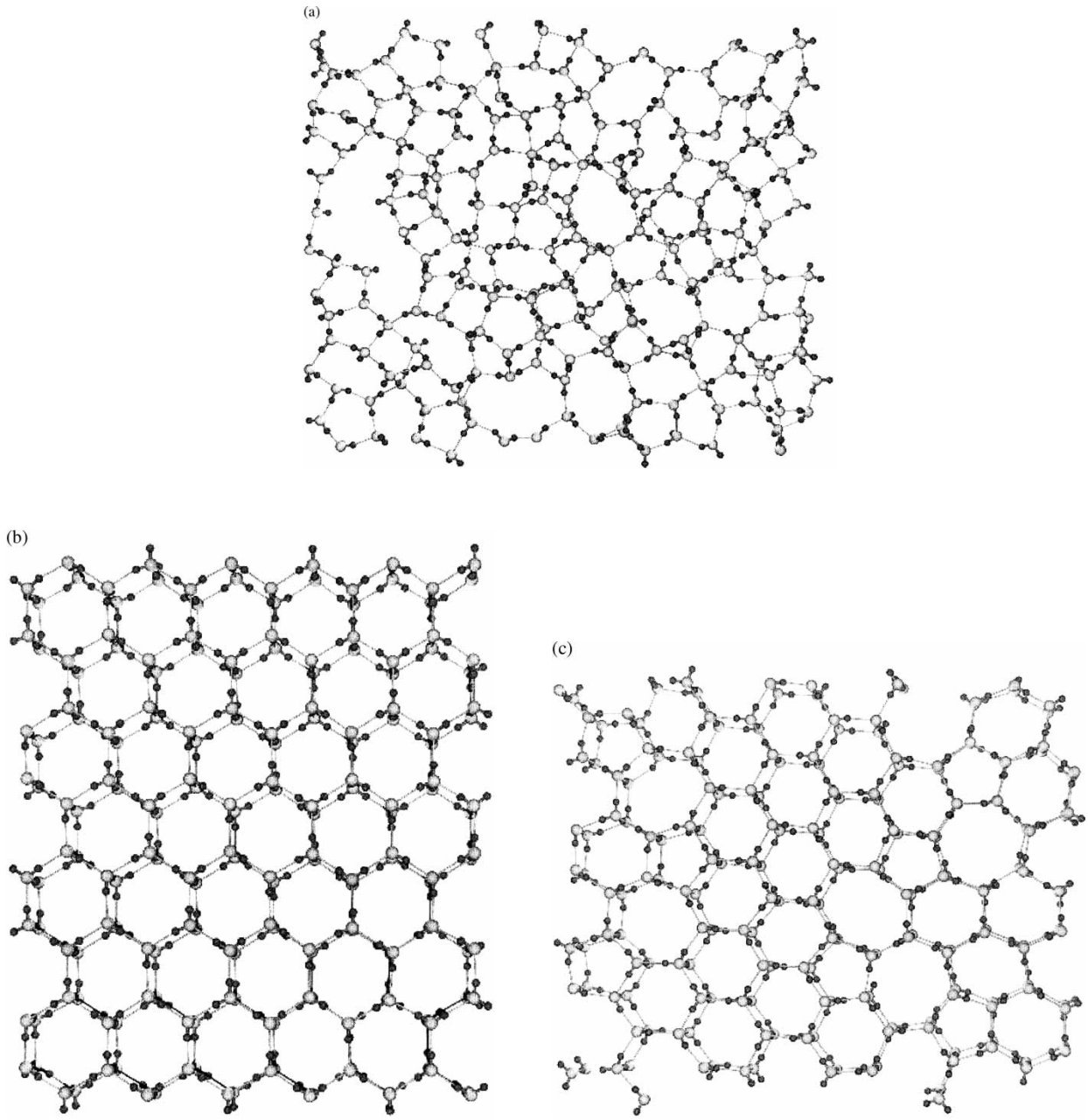

FIGURE 2 Quenched structures of the confined water in the state of (a) liquid, (b) bilayer crystal and (c) amorphous bilayer ice. Larger spheres denote oxygen and smaller spheres denote hydrogen.

the basis of the TIP4P model. However, the bilayer hexagonal ice structure obtained from the two five-site models differs somewhat from that from the four-site model. Indeed, the hexagons in both the ST2 and TIP5P bilayer crystal appear to be much less distorted than those in the TIP4P bilayer crystal. In Figs. 3–5 we show more detailed structural information for the TIP5P and ST2 bilayer ice and amorphous bilayer ice.

Figure 3a,b displays a typical geometry and the associated three O—O—O angles (α, β and γ) made by a center oxygen site with its three nearest oxygen sites in the same layer of the Q2D ice crystal. Figure 3c displays the O—O—O angle distribution for the TIP5P and ST2 bilayer crystals. It can be seen that the O—O—O angles in the TIP5P bilayer crystal exhibit five sharp peaks at 115.9°, 117.9°, 119.5°, 121.3° and 124.9°. The highest peak is located at 121.3°. However, the O—O—O angles of the ST2 bilayer crystal shows only one broad peak which is located at 120°. In contrast, for the TIP4P bilayer crystal three distinctive O—O—O angles were found, which are 108°, 118.5° and 135.5°. Based on the angle distribution for TIP4P, several bilayer ice rules were suggested. In particular, we observed that hexagons in the TIP4P bilayer crystal exhibit two orientations, which were denoted as orientation A or B. It was found that all hexagons in the same row adopt either

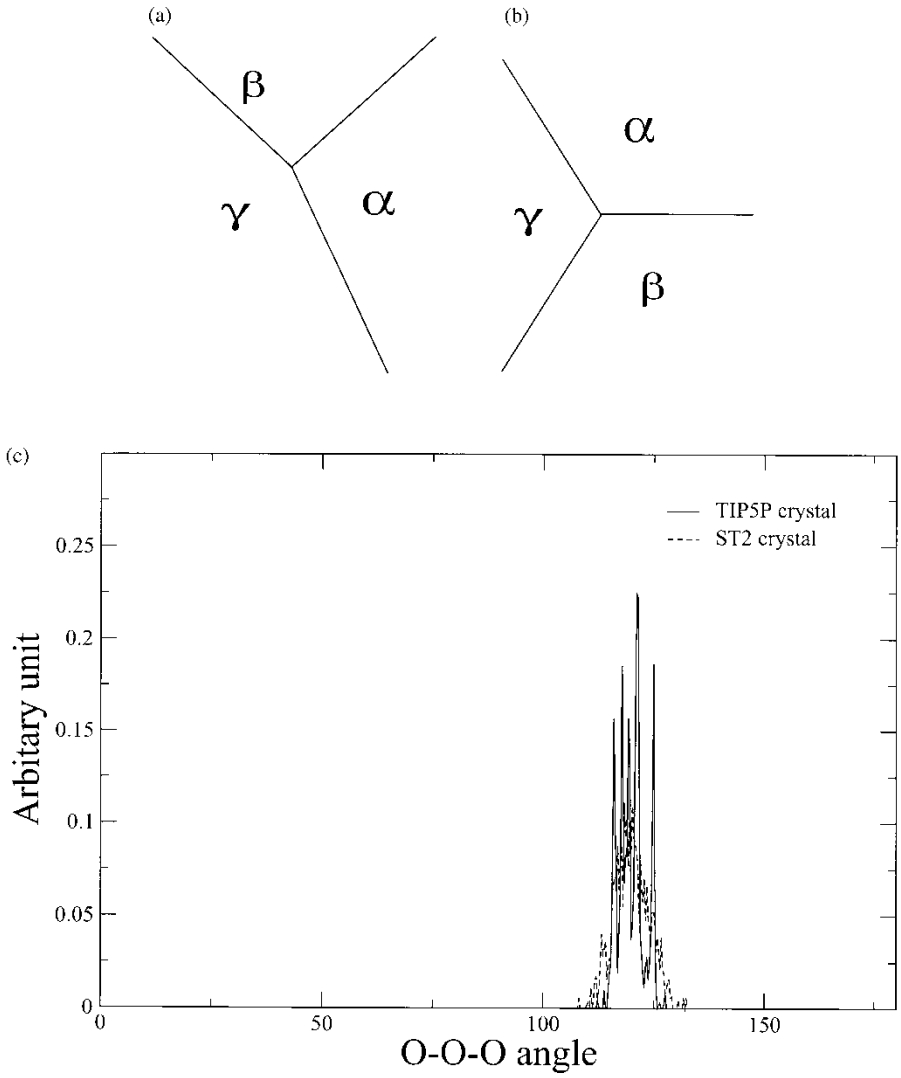

FIGURE 3 A typical geometry and the associated three O—O—O angles (α, β and γ) made by a center oxygen site with its three nearest oxygen sites in the same layer of the Q2D ice crystal. (a) For five-site models—TIP5P : $\alpha \cong \beta \neq \gamma$; ST2 : $\alpha \neq \beta \neq \gamma$; (b) For the TIP4P model [7]—$\alpha = 108°$, $\beta = 118.5°$ and $\gamma = 135.5°$. (c) The O—O—O angle distribution of TIP5P and ST2 bilayer crystals.

the orientation A or B. In the TIP4P bilayer crystal the most preferred stacking for the hexagon rows appears to be ABAB. However, for both TIP5P and ST2 bilayer crystals the O—O—O angle distribution is much narrower than that of TIP4P. In fact, the angle distribution peaks for TIP5P are located within 115° and 125° while for ST2s the peak of angle distribution is located within 110° and 130°.

Another local geometric information is the distribution of the nearest-neighbor O—O distance. For TIP5P and ST2 bilayer crystal, the distribution is shown in Fig. 4. Comparing the averaged O—O distance in the bilayer crystal to the O—O distance in water dimer (2.68 Å for TIP5P [14] and 2.74 Å for ST2 [13]) it can be found that the averaged O—O distance in the bilayer crystal is greater. In contrast, the averaged O—O distance in the TIP4P bilayer crystal is nearly the same as that in the TIP4P dimer (2.74 Å). As shown in Fig. 4, the O—O distance distribution for the two five-site models are much broader than that for the four-site TIP4P model [9,11]. These quantitative differences in local geometric configuration stems mainly from the molecular structure differences between the four-site planar model and the five-site tetrahedral model.

The two-dimensional radial distribution function was also calculated to provide global structural information of the bilayer solids. Figure 5a,b show the O—O radial distribution of TIP5P and ST2 bilayer crystal and amorphous bilayer ice, respectively. First, it can be seen that for TIP5P crystal the first peak is slightly shifted from the origin, which does not occur for the ST2 bilayer crystal. Since the first peak describes the relative location of the oxygen in the opposing layer of the crystal, it appears that the two layers of the TIP5P crystal do not exactly overlap

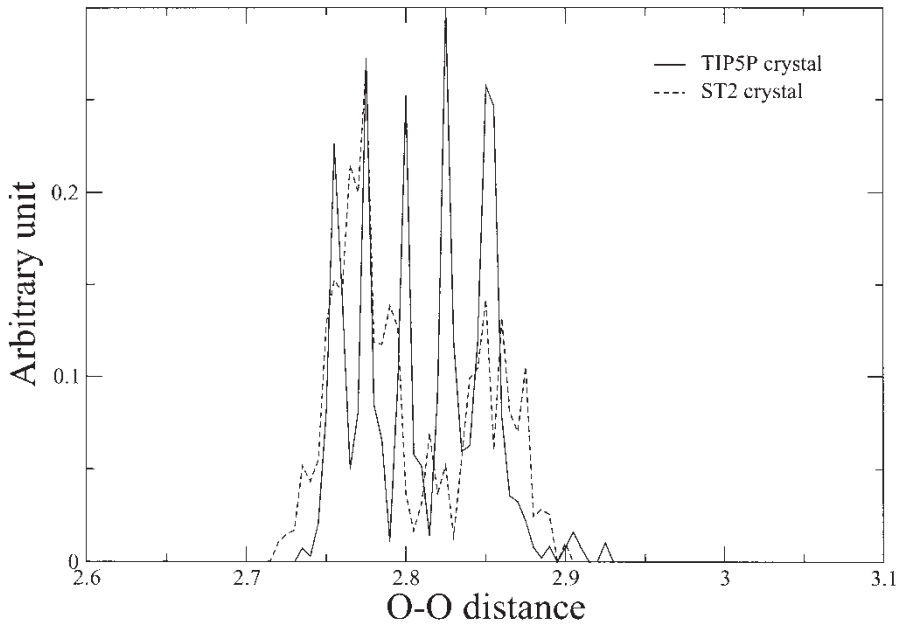

FIGURE 4 The O—O bond length distribution of TIP5P and ST2 bilayer crystals.

with each other. The O—H···O hydrogen bonding in between the two layers has typically an angle about 10° with respect to the normal (z) direction. On the other hand, the two layers of ST2 crystal nearly overlap with each other, a feature similar to the TIP4P bilayer crystal. Second, it can be seen that the location of the major peaks in the radial distribution functions is about the same for both the TIP5P and ST2 bilayer crystal, indicating the overall structure of the two bilayer crystals are about the same. However, the major peaks of TIP5P crystal are further split into a number of sharp peaks whereas those of ST2 crystal are much broader with less fine features. Moreover, the radial distribution function of the TIP5P and ST2 amorphous bilayer ice also resembles each other except the second major peak for the TIP5P amorphous ice is further split into three sharp peaks.

To summarize, our new sets of MD simulations with two five-site water models confirms our previous simulation on the basis of the four-site models [7,11], that is, in system I the bilayer ice crystal forms upon cooling whereas in system II the amorphous bilayer ice forms. A question arises: why do the two systems result in different polymorphous structure of bilayer solids? The answer to this question is still inconclusive. We have found previously that if the confined water can undergo a freezing transition into system I, the bilayer crystal is likely to form with some defects [9,10]. It seems that there exists some special numbers of water molecules when used in the simulation cell to form perfect bilayer crystals. When the number of defects is small, they can be removed by repeating several heating and cooling processes to the defected crystal. But this does not work for system II. Can it be possible to form a perfect crystal in system II under certain conditions? To explore this possibility, we performed an MD simulation with 192 ST2 molecules in system II at the same simulation conditions and with 4 ns MD time at each temperature, except we abruptly changed the temperature from 295 to 270 K (25 K change in temperature). After the amorphous bilayer ice was observed, the amorphous ice was heated from 270 K directly to either 280, 290, 295 or 300 K. When it was below 300 K, we only observed that some polygons in the amorphous ice changed into some other polygons. When it was at 300 K, however, the polygonal structure of the amorphous ice began to rearrange and eventually a hexagonal network was formed with a few defects. At this point, we increased the temperature further from 300 to 310 K and performed the MD simulation for about 0.8 ns, and then lowered the temperature directly to 280 K before the structure reached a stable configuration at 310 K. In this case, a perfect bilayer crystal was formed at 280 K after about 2 ns MD time in system II. The average potential energy of the crystal is about 0.387 kcal/mol lower than that of the amorphous ice. Therefore, once the crystal was formed, we did not detect any evidence of transformation from the bilayer crystal to amorphous bilayer ice during further heating and cooling processes. These results show that the perfect hexagonal network is very stable despite the fact that the formation of bilayer crystal is a rare event in system II. Similar behavior was found for TIP5P in system II.

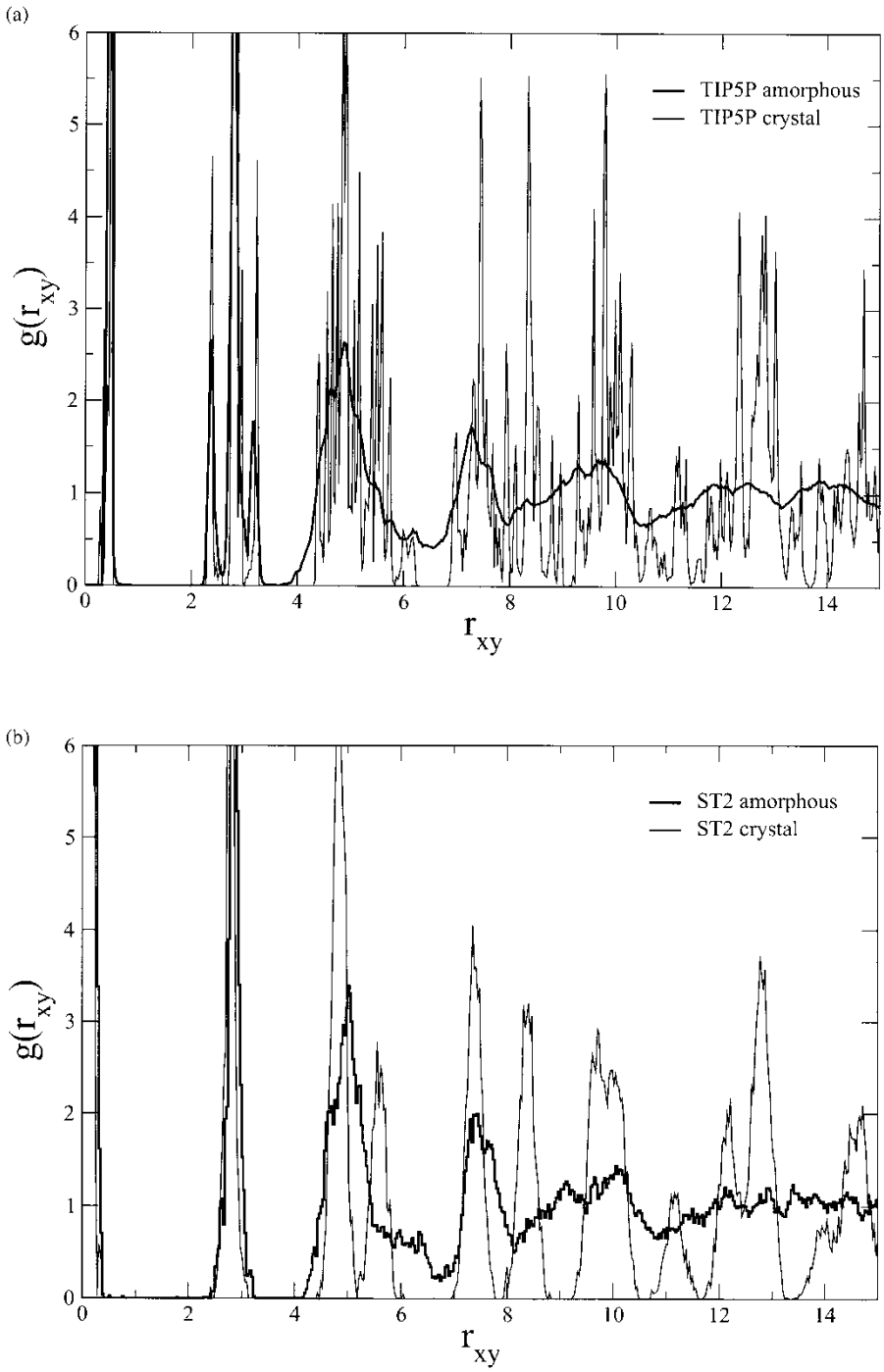

FIGURE 5 Two-dimensional radial distribution of oxygen of (a) TIP5P and (b) ST2 bilayer crystal and amorphous bilayer ice.

CONCLUSION

We have performed MD simulations of water confined to hydrophobic nanoslits to investigate the first-order phase transition phenomena. Two five-site water models, the TIP5P and ST2, were employed. Our new set of simulation confirms our previous simulations with the TIP4P model. It is found that, upon cooling, the confined water transforms into a bilayer ice crystal in system I and into an amorphous bilayer ice in system II. From the O—O distance and O—O—O angle distributions of the bilayer crystals we find that hexagons are much less distorted and thereby do not exhibit any special orientations like those in the TIP4P bilayer ice. We also find that ST2's hexagonal network is more flexible compared to the TIP4P's and TIP5P's. Finally, although the formation of a bilayer crystal is not preferred in system II, it is still conceivable to generate a bilayer crystal via multiple heating and cooling processes (somewhat like a simulated annealing). Once the bilayer crystal is formed, no

reverse process, namely, from the bilayer crystal to amorphous bilayer ice was observed, indicating that the bilayer crystal phase is indeed more stable at low temperatures even in system II. In conclusion, the computer-simulation generated Q2D bilayer ice may be considered as a possible candidate of the "Ice XIII" or whatever the next Roman numerals would be available at the time, provided that the 2D ice phases in vacuum can be recognized as a stand-alone (metastable) solid ice. Alternatively, one could introduce Roman numerals specifically for 2D ice phases. In any case, ultimate confirmation and naming of the computer-generated 2D ice structure requires crystallographic or at least spectroscopic experiments. For now, we name the 2D bilayer ice the "Nebraska ice" because according to the Otoe Indian the word "Nebraska" means "flat water" [17].

Acknowledgements

X.C. Zeng is supported by US NSF and Office of Naval Research. K. Koga and H. Tanaka are supported by the Japan Society for the Promotion of Science (JSPS) and the Japan Ministry of Education.

References

[1] Petrenko, V.F. and Whitworth, R.W. (1999) *Physics of Ice* (Oxford, New York).
[2] Mishima, O. and Stanley, H.E. (1998) "The relationship between liquid, supercooled and glassy water", *Nature* **396**, 329.
[3] Lobban, C., Finney, J.L. and Kuhs, W.F. (1998) "The structure of a new phase of ice", *Nature* **391**, 268.
[4] Gubbins, K.E., Sliwinska-Bartkowiak, M. and Suh, S.-H. (1996) "Molecular simulation of phase transitions in pores", *Mol. Simulation* **17**, 333.
[5] Gelb, L.D., Gubbins, K.E., Radhakrishnan, R. and Sliwinska-Bartkowiak, M. (1999) "Phase separation in confined systems", *Rep. Prog. Phys.* **62**, 1573.
[6] Schoen, M. (1993) *Computer Simulation of Condensed Phases in Complex Geometries* (Springer, Heidelberg).
[7] Koga, K., Tanaka, H. and Zeng, X.C. (1997) "Freezing of confined water: a bilayer ice phase in hydrophobic nanopores", *Phys. Rev. Lett.* **79**, 5264.
[8] Slovák, J., Tanaka, H., Koga, K. and Zeng, X.C. (1999) "Confined water in hydrophobic nanopores: dynamics of freezing into bilayer ice", *Phys. Rev. E* **60**, 5840.
[9] Slovák, J., Tanaka, H., Koga, K. and Zeng, X.C. (2001) "Computer simulation of water–ice transition in hydrophobic nanopores", *Physica A* **292**, 87.
[10] Slovák, J., Tanaka, H., Koga, K. and Zeng, X.C. (2003) "Computer simulation of bilayer ice: structures and thermodynamics", *Physica A* **319**, 163.
[11] Koga, K., Tanaka, H. and Zeng, X.C. (2000) "First-order transition in confined water between high density liquid and low density amorphous phases", *Nature* **112**, 8910.
[12] Jorgensen, W.L., Chandrasekhar, J., Madura, J.D., Impay, R.W. and Klein, M.L. (1983) "Comparison of simple potential functions for simulating liquid water", *J. Chem. Phys.* **79**, 926.
[13] Stillinger, F.H. and Rahman, A. (1974) "Improved simulation of liquid water by molecular dynamics", *J. Chem. Phys.* **60**, 1545.
[14] Mahoney, M.W. and Jorgense, W.L. (2000) "A five-site model for liquid water and the reproduction of the density anomaly by rigid, nonpolarizable potential functions", *J. Chem. Phys.* **112**, 8910.
[15] Steele, W.A. (1974) *Interaction of Gases with Solid Surfaces* (Pergamon Press, Oxford).
[16] Stillinger, F.H. and Webber, T.A. (1984) "Packing structures and transitions in liquids and solids", *Science* **225**, 983.
[17] Bradley, D. (2000) "Water, water…", *Alchemist*, www.chemweb.com/alchem/articles/985883672133.html.